CEBAF PROPOSAL COVER SHEET

This Proposal must be mailed to:

CEBAF
Scientific Director's Office
12000 Jefferson Avenue
Newport News, VA 23606

and received on or before OCTOBER 31, 1989

A. TITLE:

Polarization Transfer Measurements in the $D(\vec{e},e'\vec{p})n$ Reaction

B. CONTACT PERSON:

J.M. Finn

ADDRESS, PHONE AND BITNET:

Department of Physics
The College of William and Mary
Williamsburg, VA 23185
Ph #: (804) 253-4471 Bitnet: FINN@CEBAFVAX

C. THIS PROPOSAL IS BASED ON A PREVIOUSLY SUBMITTED LETTER OF INTENT

[X] YES
[ ] NO

IF YES, TITLE OF PREVIOUSLY SUBMITTED LETTER OF INTENT

same as above

D. ATTACH A SEPARATE PAGE LISTING ALL COLLABORATION MEMBERS AND THEIR INSTITUTIONS

==========

(CEBAF USE ONLY)

Proposal Received 10-31-89

Log Number Assigned PR-89-028

By KES
contact: Finn

Polarization Transfer Measurements in the $D(\vec{e},e'\vec{p})n$ Reaction

THE HALL A COLLABORATION

American University, Cal. State University LA, Case Western Reserve and LANL
Continuous Electron Beam Accelerator Facility
George Washington University, University of Georgia, Indiana University Cyclotron Facility
Kent State University, University of Maryland, Massachusetts Institute of Technology
University of New Hampshire, National Institute of Science and Technology
Norfolk State University, University of Regina, University of Rochester
University of Saskatchewan, Rutgers University, Stanford University
University of Virginia, University of Washington, College of William and Mary
NIKHEF-K, CEN Saclay, University of Clermont-Ferrand
INFN Sezione Sanita, University of Lund

Spokespersons: J.M. Finn (William & Mary), P.E. Ulmer (CEBAF)

The capabilities of CEBAF coupled with a pair of high resolution spectrometers will allow high precision measurements of polarization observables in $(\vec{e},e'\vec{p})$. These observables should provide new constraints on the nuclear structure and reaction models. We have chosen a favorable kinematics which will allow extraction of all three polarization observables at $\vec{q} = 1.26$ GeV/c. The polarization asymmetries about $\vec{q}$ will also be extracted. In another set of measurements we plan to study the q_μ^2 dependence of the reaction at zero recoil momentum. The analogous $^2H(\vec{e},e'\vec{n})p$ reaction at $p_r = 0$ is expected to provide precise information on the electromagnetic form factors of the neutron provided nuclear corrections can be handled. Our measurements will therefore test the validity of reaction models for deuterium.

Date	Description	Beam Hours	Energies	Max. Luminosity
Oct. 31, 1989	$^{1,2}H(\vec{e},e'\vec{p})$	708	1.6–4.0 GeV	$2.8\times10^{38}cm^{-2}sec^{-1}$

1 Introduction and Motivation

The (e,e′p) reaction is a powerful tool for investigating the one-body character of the nuclear response. At quasielastic kinematics the Impulse Approximation (IA) has been shown to provide a reasonable description of the knockout process. To the extent that this approximation is valid, the (e,e′p) cross section factors into a nuclear spectral function containing all the nuclear structure information times a part which describes the interaction of the electron with a constituent nucleon.[1] This simple picture thus allows the extraction of the nucleon "hole" spectral distribution from which the excitation energy spectrum of the residual nuclear system as well as the momentum distribution of bound nucleons can be determined. In addition, if the spectral function is known or fixed the (e,e′p) process can provide a characterization of the half-off-shell electron-nucleon vertex revealing information on the form of the off-shell nucleon current operator as well as the electromagnetic form factors of nucleons embedded in the nuclear medium. Such information is crucial to a complete understanding of the reaction. There is no unambiguous method for extrapolating theoretical nucleon models off the mass shell[2] and, thus, experimental input is vital to our understanding of medium modified nucleons. This knowledge is clearly essential if one is to have a complete understanding of the (e,e′p) reaction for complex nuclei. Clearly, spin degrees of freedom are an important missing ingredient in constraining the reaction mechanism.

In recent years the theory of the spin structure of the electromagnetic current has been developed in some detail in anticipation of the new high duty factor electron facilities. Among others, Donnelly has developed a theoretical framework for studying polarization experiments including electron beam helicity, target and recoil polarization and photon angular correlation measurements.[3] A detailed analysis of the polarization response functions in $(\vec{e},e'\vec{p})$ has been developed by Picklesimer and Van Orden.[4] Their analysis shows that there are 18 independent response functions in the general case, for a polarized electron beam, involving

proton polarization and non-coplanar kinematics:

$$\begin{aligned}\frac{d^3\sigma}{d\omega d\Omega_e d\Omega_p} = \frac{m|\vec{p}'|}{2(2\pi)^3}\left[\frac{d\sigma}{d\Omega_e}\right]_{Mott} \times \{ & v_L(R_L + R_L^n S_n) + v_T(R_T + R_T^n S_n) \\ & + v_{TT}\left[(R_{TT} + R_{TT}^n S_n)\cos 2\phi_x + (R_{TT}^l S_l + R_{TT}^t S_t)\sin 2\phi_x\right] \\ & + v_{LT}\left[(R_{LT} + R_{LT}^n S_n)\cos\phi_x + (R_{LT}^l S_l + R_{LT}^t S_t)\sin\phi_x\right] \\ & + hv_{LT'}\left[(R_{LT'} + R_{LT'}^n S_n)\sin\phi_x + (R_{LT'}^l S_l + R_{LT'}^t S_t)\cos\phi_x\right] \\ & + hv_{TT'}(R_{TT'}^l S_l + R_{TT'}^t S_t)\}.\end{aligned} \tag{1}$$

The response functions, R, depend on $\vec{q}$, ω, T_p (the proton kinetic energy) and θ_x (the proton angle with respect to $\vec{q}$). ϕ_x is the angle between the electron scattering plane and the plane containing $\vec{q}$ and the detected proton. The v's are known kinematic factors weighting the various virtual photon polarization states and $[d\sigma/d\Omega_e]_{Mott}$ is the cross section for scattering from a structureless Dirac particle. The S's are the three components of a unit vector pointing along the proton spin direction. For coplanar kinematics the *polarization dependent* part of the cross section simplifies to:

$$\begin{aligned}\frac{d^3\sigma}{d\omega d\Omega_e d\Omega_p} = \frac{m|\vec{p}'|}{2(2\pi)^3}\left[\frac{d\sigma}{d\Omega_e}\right]_{Mott} \times & \\ \{ & \left[v_L R_L^n S_n + v_T R_T^n S_n + v_{TT} R_{TT}^n S_n \cos 2\phi_x\right] \\ & + v_{LT} R_{LT}^n S_n \cos\phi_x \\ & + hv_{LT'} R_{LT'}^l S_l \cos\phi_x \\ & + hv_{LT'} R_{LT'}^t S_t \cos\phi_x \\ & + hv_{TT'} R_{TT'}^l S_l \\ & + hv_{TT'} R_{TT'}^t S_t\}.\end{aligned} \tag{2}$$

For coplanar kinematics since only the normal polarization component is helicity independent, all three polarizations can be separated in a single measurement, assuming a favorable spin precession angle. In addition, by making measurements on either side of $\vec{q}$ one can separate the even and odd contributions.

A fundamental understanding of the nuclear current begins with understanding the electromagnetic form factors of the underlying nucleonic degrees of freedom and then by understanding the character of the nucleon–nucleon interaction. The latter is best revealed by studying the only fundamental two-body system, the deuteron.

These elementary systems provide essential constraints for understanding more complex systems.

Naturally, a characterization of the free nucleon form factors is of paramount importance both for its own sake and as a starting point for realistic off-shell nucleon models. The neutron electric form factor is practically undefined by the present data. Furthermore, beyond q_μ^2=1 (GeV/c)^2 the proton electric form factor is also badly known. So far, nucleon form factors have been extracted with Rosenbluth separation techniques. The longitudinal cross section is proportional to G_E^2 and thus provides a measure of the electric form factor. However, at high momentum transfers the scattering process is predominantly transverse and so the uncertainties on G_E using this method are quite large. By contrast, a measurement of polarization transfer in ($\vec{e}$,e'$\vec{p}$) or ($\vec{e}$,e'$\vec{n}$) can provide a much more accurate determination of G_E. At quasifree kinematics in the Impulse Approximation, the transverse polarization component is proportional to the product $G_E G_M$ rather than G_E^2.[5] A measurement of G_E^n using this technique at a single momentum transfer is planned for the Bates laboratory.[6] Detailed analyses by Arenhövel[7] and Korchin *et al.*[8] indicate that the experiment should be remarkably insensitive to the details of the nuclear model including the choice of wavefunction, FSI and MEC's.

As one moves away from the quasielastic peak, model dependences can become significant, as indicated by a calculation of Arenhövel[7] as shown in Figure 1. In particular, the normal component of polarization which vanishes in the IA can be quite large when FSI are included. Rekalo *et al.* have published a relativistic IA calculation of the dominant helicity dependent amplitudes in the kinematic domain relevant to CEBAF.[9] Their calculation of the proton transverse polarization component in D($\vec{e}$,e'$\vec{p}$)n for four momentum transfers from $q_\mu^2 = 0.5$ to 2 GeV^2/c^2 is shown in Figure 2. Although the analysis is incomplete since it neglects important ingredients such as FSI and MEC, it indicates that significant polarizations and polarization asymmetries can be expected. Complete relativistic calculations are underway by Gross and Van Orden.[10]

In this proposal we describe a first set of measurements to determine the polarization response functions in D($\vec{e}$,e'$\vec{p}$)n. A measurement of the angular distribution of

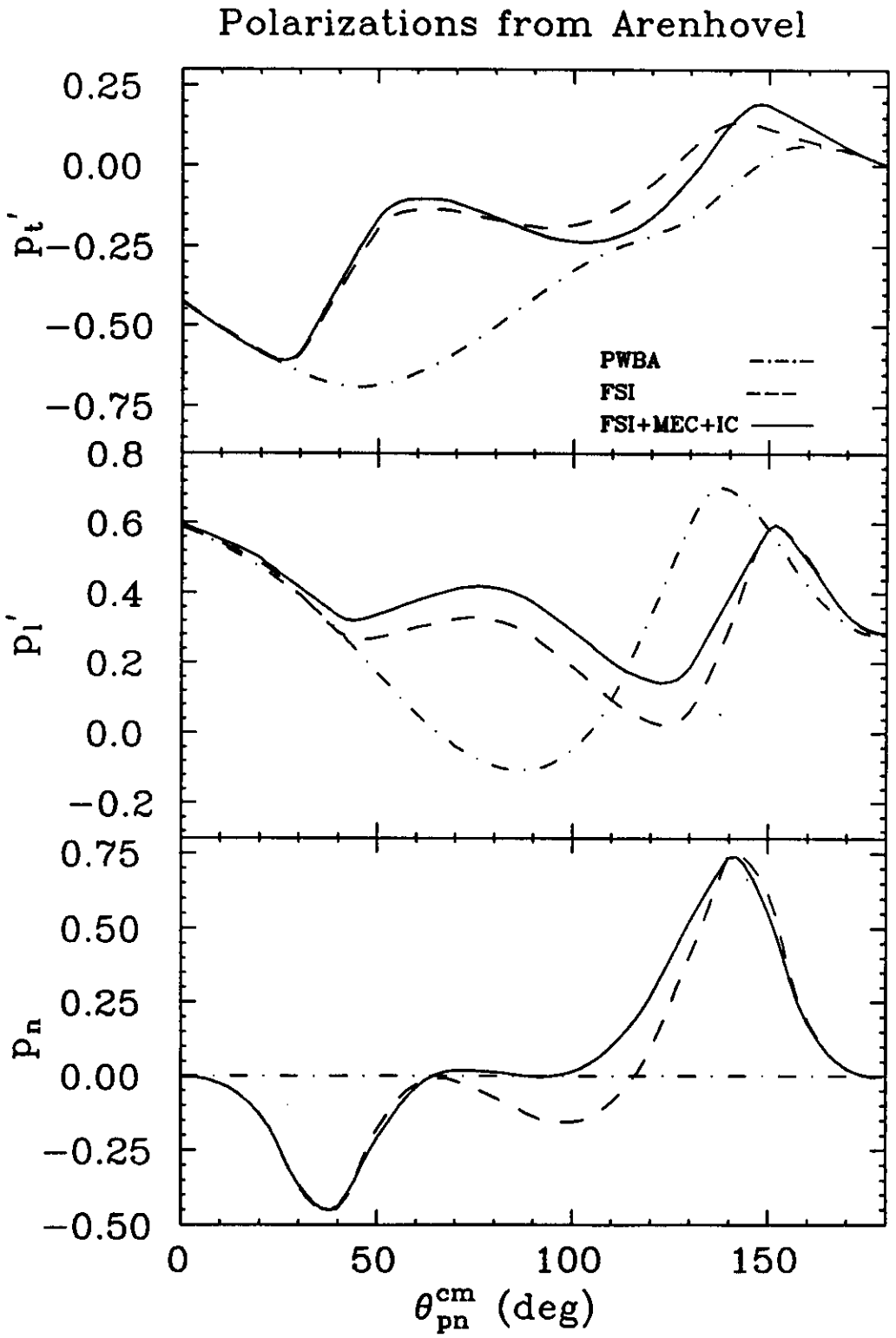

Figure 1 Polarization observables for $^2H(\vec{e},e'\vec{p})n$ as calculated by Arenhövel for an incident electron energy of 899 MeV and electron scattering angle of 60°.

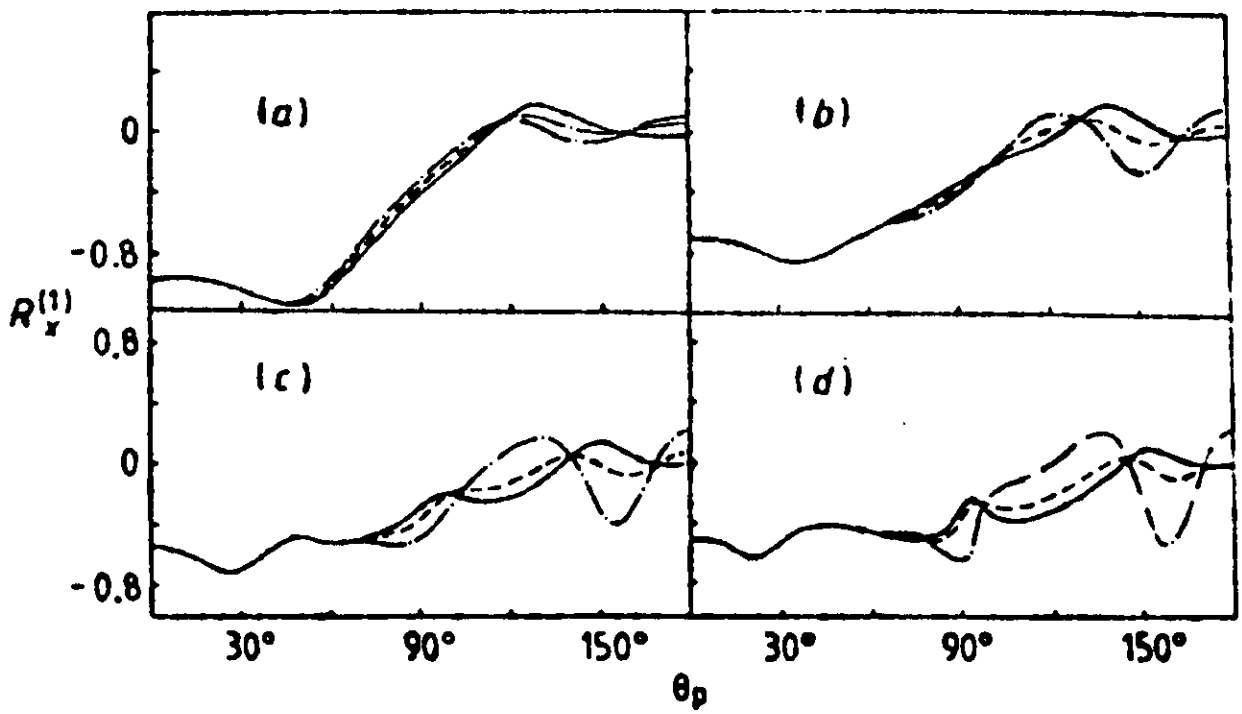

Figure 2 Calculation of Rekalo *et al.* for the transverse polarization component (divided by the transverse cross section, σ_T) for various G_E^n parameterizations. The four kinematics shown correspond to q_μ^2 (in GeV^2/c^2) and E_{pn}^{cm} (in MeV) respectively of (a) 0.5 and 128; (b) 1 and 250; (c) 1.5 and 365; (d) 2 and 473.

the polarization response will provide important constraints on the nuclear model. We have chosen the kinematics to optimize the extraction of all three polarization amplitudes by picking a proton energy such that the normal and longitudinal components are precessed by 45° in the vertical bending HRS magnets. The normal component is helicity independent and can therefore be separated from the other two components. In addition, by making in-plane measurements to the right and left of $\vec{q}\,(\phi_x = 0, \pi)$, the polarization asymmetries can be measured. By use of high luminosities, a recoil momentum of 300 MeV/c can be reached which is significant on the scale of the maximum of the S and D state interference.

Another set of measurements will examine the q_μ^2 dependence of the $(\vec{e},e'\vec{p})$ response at the top of the quasielastic peak. Since the neutron electric form factor is poorly known the analogous $(\vec{e},e'\vec{n})$ experiment will be unable to distinguish between interaction effects and differences in G_E^n. However, such model dependences may be examined using the proton knockout reaction ^{2}H$(\vec{e},e'\vec{p})$n. We

propose to measure this reaction for several momentum transfers from $\vec{q}$ = 0.5 GeV/c to $\vec{q}$=2.5 GeV/c at zero recoil momentum. Such a systematic study will provide a sensitive test of deuteron models and should also stimulate the activity of theoretical groups able to do relativistic calculations. This set of measurements should logically be performed at the same time as proposed measurements of G_E^p via p($\vec{e}$,e'$\vec{p}$).[11]

It is clear that measurements of polarization observables will play an important role at CEBAF where the high duty factor will make statistically precise measurements possible. Indeed, such measurements are required for a complete determination of all the electromagnetic nuclear structure functions.[12]

2 The Experiment

The experiment involves measuring the polarization of a proton after being scattered quasielastically by a longitudinally polarized electron. What is measured is the proton spin orientation relative to the incident electron helicity. For the special case of parallel kinematics (protons detected along $\vec{q}$), assuming the interaction conserves angular momentum and parity, there are three polarization structure functions which survive. Two of these, p_l' and p_t', require a polarized electron beam; the third, p_n, is an induced polarization and is helicity independent. The transverse component of the recoil proton polarization (i.e. the component in the scattering plane and perpendicular to the proton momentum), p_t', is related to the electron beam helicity, h, as:

$$p_t' = hD_{lt}. \tag{3}$$

The longitudinal component (i.e. along the proton momentum direction) is given by

$$p_l' = hD_{ll}. \tag{4}$$

Here, the D's represent the polarization transfer coefficients. (In parallel kinematics the polarization transfer component normal to the electron scattering plane, p_n', is zero.) Arenhövel predicts that at $p_r = 0$ the two components of polarization

in the scattering plane are very nearly the same as for elastic ep scattering.[7] These can be written in terms of the elementary nucleon form factors, G_E and G_M:[5]

$$\begin{aligned} I_0 D_{lt} &= -2\sqrt{\tau(1+\tau)} G_M G_E \tan\theta_e/2 \\ I_0 D_{tt} &= \frac{(e_0 + e')}{m} \sqrt{\tau(1+\tau)} G_M^2 \tan^2\theta_e/2 \end{aligned} \tag{5}$$

where

$$I_0 = G_E^2 + \tau G_M^2 \left[1 + 2(1+\tau)\tan^2\theta_e/2\right] \tag{6}$$

and e_0 (e') is the electron initial (final) energy, θ_e is the electron scattering angle, m is the proton mass and $\tau = q_\mu^2/4m^2$. The spin component from which G_E is extracted is transverse and thus does not precess in a vertically bending spectrometer. In addition, although for parallel kinematics in IA no proton polarization can occur for unpolarized electrons, an induced polarization normal to the electron scattering plane will result from np final state interactions; such a component will also be affected by the presence of MEC's and IC's. The Arenhövel prediction for this component is very small in the $\vec{q}$ direction, but reaches measurable size for $\theta_{pn}^{cm} > 30°$ (where θ_{pn}^{cm} is the proton angle relative to $\vec{q}$ in the final np center of mass system). Note that FSI may produce large normal polarizations on complex nuclear systems.[13]

For general coplanar kinematics one can determine polarization asymmetries as well. These asymmetries are characterized by a $\cos\phi_x$ dependence in the corresponding response functions and therefore change sign on either side of $\vec{q}$. By constructing sums and differences of the polarization response, one can extract six different observables for fixed electron kinematics (the six observables are each given on a separate line of Eq. 2).

As mentioned above, the transverse polarization component does not precess to first order. On the other hand, the normal and longitudinal components precess about the spectrometer magnetic field direction. Thus, in general, the polarimeter is capable of measuring the transverse component as well as a mixture of the longitudinal and normal components. However, because in parallel kinematics the longitudinal polarization is helicity dependent while the normal term is helicity independent, under favorable conditions both the normal and longitudinal components can be separated. In the polarimeter coordinate system (X axis along the

momentum dispersion direction, Y axis normal to the bend plane and Z axis along the proton momentum direction) we have for the components of polarization after precession by an angle χ through the spectrometer:

$$\begin{aligned} p_X &= p_n \cos\chi + p_l \sin\chi \\ p_Y &= p_t \\ p_Z &= -p_n \sin\chi + p_l \cos\chi. \end{aligned} \tag{7}$$

The precession angle is given by

$$\chi = \frac{g-2}{2}\gamma\Omega_B \tag{8}$$

where g is the proton gyromagnetic ratio (=5.586), γ is the Lorentz factor ($= E_p/m$) and Ω_B is the total bend angle for the spectrometer central ray.

Arenhövel has calculated polarization observables for the ^{2}H($\vec{e}$,e'$\vec{p}$)n reaction. His results for an incident electron energy of 899 MeV and electron scattering angle of 60° are shown in Figure 1. The polarization amplitudes which are not shown in the figure vanish for coplanar kinematics. These calculations are nonrelativistic and for much lower energies than for the measurements being discussed here, but they are the only realistic calculations currently available and serve to illustrate the relevant points. For zero recoil momentum, $\theta_{pn}^{cm} = 0$, the effects of FSI, MEC and IC are predicted to be quite small. The longitudinal component of polarization (which is measurable due to the spin precession in the spectrometer) is similar in magnitude to the expected value of the transverse component. The normal component can also be separated but, according to Arenhövel's calculation, the expected value is quite small. However, in contrast to the l and t components which are expected to be predominantly one-body in character, the n component is zero in the absense of np final state interactions.

3 q_μ^2 Dependence Study

In order to test the validity of various reaction models for deuterium, we plan to measure the D($\vec{e}$,e'$\vec{p}$)n reaction at quasifree kinematics. These kinematics are similar to those for the analogous D($\vec{e}$,e'$\vec{n}$)p experiment to extract G_E^n. The kinematics are centered at p_r=0 and will provide a study of the q_μ dependence of the

reaction; they are given in Table 1. A minimum angle of 13.7° for the electron arm and a maximum beam energy of 4 GeV have been assumed. The precession angle, χ, is also given in Table 1 (assuming a spectrometer bend angle of 45°). Since the longitudinal polarization depends on the incident electron helicity whereas the normal component does not, both the longitudinal and normal components can be determined for favorable precession angles. The proton form factors and polarizations obtained with the dipole model are shown in Table 2 for each kinematics.

Table 1
Kinematics

Kin	e_0 GeV	$\vec{q}$ GeV/c	E_{np}^{cm} MeV	ω MeV	T_p MeV	θ_e deg	θ_p deg	χ deg
1	1.600	0.5	62	127.1	124.9	18.12	−66.40	91
2	4.000	1.0	206	435.2	433.0	13.69	−57.55	118
3	4.000	1.5	378	833.2	831.0	20.19	−46.75	152
4	4.000	2.0	554	1273.1	1270.9	27.01	−38.26	190
5	4.000	2.5	727	1734.2	1732.0	34.80	−31.15	230

Table 2
Form Factors and Polarizations (Dipole)

Kin	q_μ^2 (GeV^2/c^2)	G_E^p	G_M^p	D_{lt}	D_{ll}
1	0.23	0.566	1.58	−0.127	0.0925
2	0.81	0.218	0.609	−0.136	0.185
3	1.56	0.0981	0.274	−0.167	0.317
4	2.38	0.0528	0.148	−0.196	0.471
5	3.24	0.0323	0.0902	−0.214	0.625

Count rate estimates were made assuming the spectrometer acceptances given in Table 3. For the singles rate estimates the full acceptances are considered. In addition, the rates with a cut on ω corresponding to the maximum of the quasielastic peak were also calculated. The accidentals rates are calculated assuming cuts in

Table 3

Assumed Spectrometer Acceptances

Quantity	Electron Arm	Proton Arm
momentum	±5%	±5%
θ_V	±65 mr	±65 mr
θ_H	±30 mr	±30 mr

missing mass (a resolution of 1 MeV is assumed), ω and making use of the excellent vertex resolution (± 1 mm) of the spectrometer pair.

The (e,e′) cross sections were calculated with the computer code, QFSV[14] which employs a Fermi gas model to compute the quasielastic component and includes contributions from the delta and higher resonances. The cross sections integrated over the momentum acceptance of the electron arm are given in Table 4 without cuts as well as with a cut on ω corresponding to the region of the quasielastic peak. Counting rates are given in Table 5 and assume a luminosity of 150 μA-g/cm^2.

Table 4

Integrated Single-Arm Cross Sections

Kinematics	(e,e′) nb/sr	(e,e′) w/ ω cut nb/sr	(e,π^-) nb/sr	(e,p) nb/sr	(e,π^+) nb/sr
1	1480	1250	6.70	56.8	16.2
2	186	146	15.5	39.6	26.8
3	8.21	7.84	14.7	624	29.1
4	0.827	0.801	14.1	422	25.4
5	0.167	0.129	13.3	335	10.5

The (e,p), (e,π^+) and (e,π^-) cross sections were calculated with the electroproduction code, EPC.[14] The (e,p) cross section is approximated by the (γ,p) cross section times a factor corresponding to the virtual photon flux:[15]

$$\frac{d^2\sigma}{d\Omega_p dE_p} = \frac{N_e(\omega)}{\omega_0} R \frac{d\sigma_\gamma}{d\Omega_p} \tag{9}$$

This assumes the dominance of the transverse component and the forward peaking approximation (FPA) since most virtual photons arise from near 0° scattering of

Table 5

Single-Arm Counting Rates (Hz)

Kinematics	(e,e′)	(e,e′) w/ ω cut	(e,π^-)	(e,p)	(e,π^+)
1	3300000	2800000	15000	130000	36000
2	410000	320000	34000	87000	59000
3	18000	17000	33000	1400000	65000
4	1800	1700	32000	930000	56000
5	380	280	30000	740000	23000

the electron. Here, R is a recoil factor and ω_0 is the energy transfer in the FPA. $N_e(\omega)$ is the virtual photon spectrum. For deuterium the (γ,p) cross section for scattering to the pn channel is taken from a fit to deuteron photodisintegration data.[16] For the quasifree pion production region a Breit-Wigner form was used in the delta region with appropriate angular dependences, and above that the cross section was assumed to be uniform and isotropic in the center-of-mass frame. Integrated cross sections and singles rates are given in Tables 4 and 5 respectively.

The (e,e′p) cross sections were calculated with the computer code MCEEP.[17] This code performs a folding of the cross section over the experimental acceptances and gives realistic count rate estimates for any desired kinematical cut. It also evaluates systematic and statistical contributions to the experimental uncertainties. The nuclear model used for the present count rate estimates assumes the validity of the Plane Wave Impulse Approximation (PWIA); thus, the (e,e′p) cross section factors into an elementary ep off-shell cross section times a quantity which contains the nuclear structure information, the spectral function:[1]

$$\sigma_{eep} = K\sigma_{ep}\frac{1}{\eta}S(\vec{p}_r, \epsilon_m) \tag{10}$$

where K is a kinematical factor. The recoil factor, η, for scattering to a bound state of the residual nucleus is given by

$$\eta = 1 - \frac{E_p}{E_r}\frac{\vec{p}\,' \cdot \vec{p}_r}{|\vec{p}\,'|^2} \tag{11}$$

where $E_{p(r)}$ is the total energy of the detected proton (recoiling system) and $\vec{p}\,'$ is the proton final momentum. The spectral function, S, represents the joint probability for finding within the nucleus a proton of momentum $-\vec{p}_r$ and separation energy ϵ_m. All of the dependence on virtual photon polarization is contained

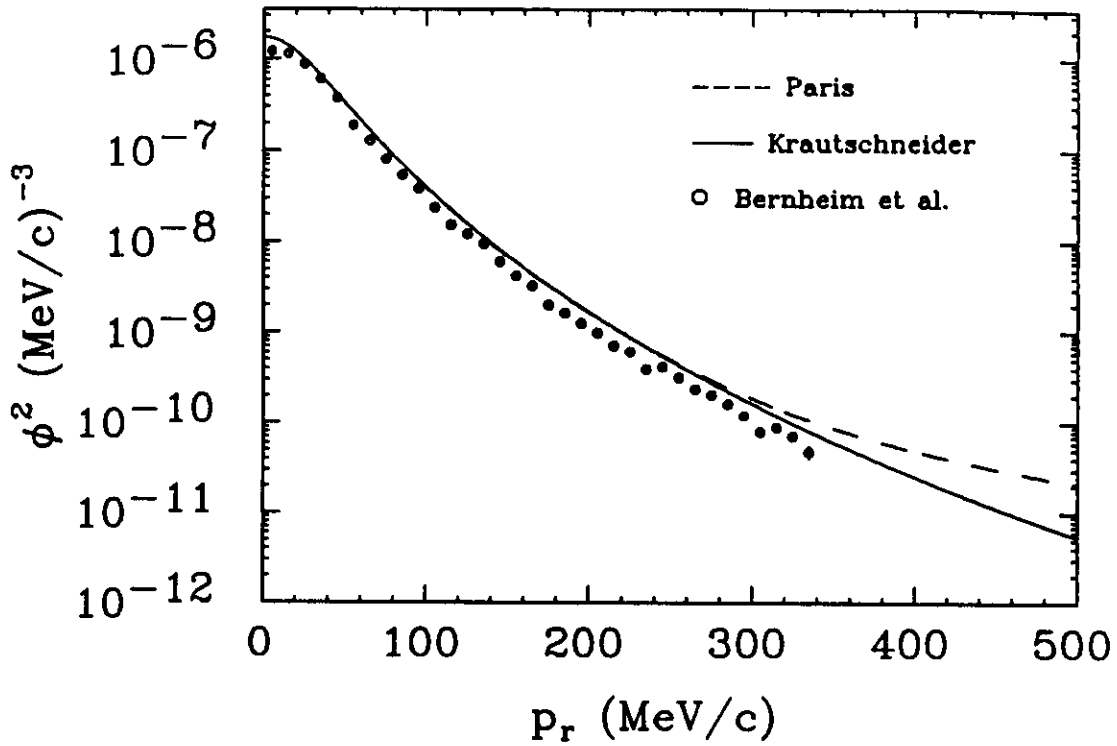

Figure 3 Deuteron momentum distribution as measured by Bernheim *et al.*[19] Also shown are the Krautschneider and Paris parameterizations.

within the *ep* cross section. Many ambiguities exist in the extrapolation of the on-shell cross section to that for a bound proton. However, all prescriptions are fairly consistent for protons which are nearly on-shell. Here, the "CC1" prescription of de Forest is used for σ_{ep}.[2] The bound state spectral function is given by

$$S(\vec{p}_r, \epsilon_m) = |\phi(p_r)|^2 \delta(\epsilon_m - \epsilon_b) \tag{12}$$

where ϵ_b is the binding energy (=2.2 MeV for deuterium). The $|\phi(p_r)|^2$ are taken from the parameterization of Krautschneider:[18]

$$|\phi_D(p_r)|^2 = 4\pi N \left(\frac{1}{T_1} - \frac{1}{T_2}\right)^2 \tag{13}$$

with

$$\begin{aligned} T_1 &= p_r^2 + k_1 \\ T_2 &= p_r^2 + k_2. \end{aligned} \tag{14}$$

The constants $k_1 = 2088$ (MeV/c)^2 and $k_2 = 67600$ (MeV/c)^2 reproduce the shape of the experimental distribution up to $p_r \sim 300$ MeV/c quite well. The distribution was normalized to yield one proton (N=0.638 MeV/c). Figure 3 compares this shape with the data of Bernheim *et al.*[19] Also shown in the figure is the deuteron momentum distribution derived from the nucleon-nucleon interaction of the Paris potential.[20] Below p_r=300 MeV/c the Paris and Krautschneider parameterizations are nearly identical.

Coincidence rates with and without cuts are given in Table 6. Accidentals rates assume a coincidence resolving time of 2 ns base width and reflect cuts in missing mass, ω and a test for a consistent coincidence vertex. The raw signal to noise ratio is so favorable for all cases that it is not explicitly tabulated.

Table 6

Coincidence Rates

Kin	ω range MeV	$\lvert p_r \rvert$ range MeV/c	trues sec^{-1}	accid sec^{-1}
1	54–201	full	98000	
	111–143	0–30	42000	3.03
2	257–613	full	16000	
	403–467	0–30	2700	0.087
3	675–992	full	2600	
	785–881	0–30	380	0.050
4	1137–1409	full	650	
	1209–1337	0–30	96	0.0025
5	1621–1848	full	170	
	1654–1814	0–30	33	0.00026

In addition to kinematical cuts, one must consider only those coincident events which scatter usefully in the focal plane polarimeter. The cross section for scattering a polarized electron from an unpolarized proton followed by a second scattering of the outgoing polarized proton from an analyzer is (for parallel kinematics):[21]

$$\sigma = \sigma_0 \left[1 + p'_t A_y \sin\phi_2 + \left(p_n \cos\chi + p'_l \sin\chi\right) A_y \cos\phi_2\right] \tag{15}$$

where ϕ_2 is the azimuthal angle of the secondary scattering, A_y is the analyzing power, σ_0 is the unpolarized cross section and χ is the precession angle in the proton spectrometer. By measuring the ϕ_2 distribution in the polarimeter one can extract, through Fourier analysis, the polarization components p'_t, p'_l and p_n. The absolute statistical uncertainty in each polarization component is

$$\Delta p = \frac{\pi}{2\overline{A_y}}\sqrt{\frac{1}{fN}} \tag{16}$$

where $\overline{A_y}$ is the analyzing power averaged over an angular cone for which A_y is substantially different than zero (proton angles greater than $\sim 3°$), f is the fraction

of events which scatter into this cone and N is the total number of events detected in the spectrometer focal plane. Shown in Table 7 are the polarimeter figures of merit for each kinematics. The numbers given are reasonable extrapolated values from recent measurements at Saturne.[22] Since this experiment involves measuring an asymmetry with respect to the incident electron helicity most of the systematic errors cancel.

Table 7
Polarimeter Figures of Merit

Kin	$f\overline{A_y}^2$ $\times 10^{-3}$
1	0.63
2	17.5
3	9.8
4	6.6
5	5.3

Shown in Table 8 are the counting times and resulting absolute statistical uncertainties in $D_{lt} = p'_t/h$ assuming a luminosity of $2.8\times10^{38}\text{cm}^{-2}\text{sec}^{-1}$ and a beam polarization of 40%. The total acquisition time for the q_μ dependence study is 248 hours. A beam polarization of 80% will reduce this time estimate by a factor of four.

Table 8
Counting Times

Kin	δD_{lt} (absolute)	time (hours) $L_{\text{max}} = 150\mu\text{A-g/cm}^2$
1	0.01	1.62
2	0.01	0.91
3	0.01	11.5
4	0.01	67.6
5	0.015	109
TOTAL		191
TOTAL after rad. corr.		248

4 Angular Distribution Study

For the angular distribution study we plan to work at a fixed electron kinematics (see Table 9) and measure the proton yield as a function of the opening angle relative to $\vec{q}$. Measurements on either side of $\vec{q}$ will allow a separation of the odd and even response functions up to a recoil momentum of 300 MeV/c. The momentum transfer was chosen to give a precession angle of 135° which optimizes the simultaneous extraction of the normal and longitudinal components for a 45° vertical bend spectrometer.

Table 9
Kinematics for Angular Distribution Measurement

$\vec{q}$ GeV/c	e MeV	ω MeV	θ deg	ϵ
1.259	4000.0	634.1	17.05	0.943
Kin	p_r MeV/c	T_p MeV	θ_p deg	θ_{cm}^{pn} deg
0	0	631.9	−51.60	0
50A	50	630.5	−49.33	5.27
50B			−53.88	
100A	100	626.6	−47.05	10.51
100B			−56.16	
150A	150	620.0	−44.77	15.78
150B			−58.44	
200A	200	610.9	−42.47	21.04
200B			−60.73	
250A	250	599.2	−40.17	26.30
250B			−63.03	
300A	300	585.2	−37.86	31.57
300B			−65.35	

The experimental methodology is the same as described in the previous section. However, since the electron arm is fixed it also provides a useful relative luminosity monitor for these measurements. Tables 10 and 11 show the energy-integrated single-arm cross sections and rates respectively. Coincidence rates are shown in

Table 11 as well. Counting times are based on extraction of the even (e) and odd (o) components of the transverse polarization transfer coefficient, $\delta D_{lt}^{e,o}$, to a statistical precision of 0.01 except for the highest recoil momentum point where it is 0.015. The number of counts required per measurement, N, for a given accuracy in $D_{lt}^{e,o}$ is given by

$$(\delta D_{lt}^{e,o})^2 = \frac{\pi^2}{8h^2\overline{A_y}^2 fN}$$

where

$$D_{lt}^{e,o} = [D_{lt}(\phi_x = 0) \pm D_{lt}(\phi_x = \pi)]/2.$$

The determination of the longitudinal coefficient is less accurate by a factor of $\sqrt{2}$ because of the precession angle of 45°. The same factor occurs for the normal component but this is compensated for by its helicity independence. Counting times are shown in Table 11 assuming a beam polarization of 40%. Total acquisition time after radiative corrections is estimated at 393 hours.

Table 10

Cross Sections for $|\phi(p_r)|^2$ Measurement

$\sigma_{ee'} = 37.7$ nb/sr

$\sigma_{e\pi^-} = 15.4$ nb/sr

Kin	(e,p) nb/sr	(e,π^+) nb/sr
0	846	28.1
50A	964	28.8
50B	757	27.4
100A	1040	29.5
100B	718	26.6
150A	1030	29.8
150B	677	24.4
200A	819	30.6
200B	651	14.7
250A	575	30.9
250B	622	6.10
300A	274	31.3
300B	598	0

Table 11

Counting Rates for Angular Distribution

(e,e′) Rates: 82900 sec^{-1}

(e,π^-) Rates: 34000 sec^{-1}

Kinematics	(e,p) sec^{-1}	(e,π^+) sec^{-1}	trues sec^{-1}	accidentals sec^{-1}	S/N	time hours
0	1860000	30100	5800	309	28200	0.3
50A	2120000	63400	7660	352	16400	0.4
50B	833000	60400	3940	276	21400	0.4
100A	2280000	65000	1180	379	4690	1.4
100B	1580000	58600	1350	262	7730	1.2
150A	2280000	65600	290	377	1150	5.5
150B	1490000	53800	387	247	2350	4.1
200A	1800000	67400	73.8	299	370	21.5
200B	1430000	32200	128	238	810	12.4
250A	1270000	68000	20.7	210	148	76.7
250B	1370000	13400	48.6	227	321	32.6
300A	602000	69000	6.43	100	96.4	109.7
300B	1320000	0	19.7	218	135	35.8
TOTAL						302
TOTAL after rad. corr.						393

5 Experimental Equipment

In addition to the standard Hall A coincidence setup which consists of the two high resolution spectrometers, we will require both a polarized beam and a recoil polarimeter in the hadron arm. We also require high power liquid deuterium and hydrogen targets.

In order to maintain a favorable signal-to-noise ratio at high recoil momenta, good missing mass and vertex resolution are required. The dynamic range of this experiment requires spectrometers with a momentum range of $\sim$ 1 GeV/c to 4 GeV/c with a premium on reaching small angles.

For the standard electronics we plan to use pairs of vertical drift chambers to

determine the final particle trajectories. Because of the rapid variation of the coincidence cross section across the acceptance, the focal plane must be uniform and well understood. Additional instrumentation is required for accurate timing and particle identification. In particular, pion rejection in the electron arm will require the use of both Čerenkov and shower counters.

To minimize running times, high luminosity and the ability to view extended targets is required. The Hall A collaboration is developing high power liquid targets capable of sustaining full beam current on an extended target cell of 10–15 cm. In addition, we will need to have CH_2 and ^{12}C targets in the ladder for additional normalization checks. Also, a BeO screen will be required for alignment checks.

A major part of the effort will involve constructing and testing a focal plane polarimeter. A baseline design uses horizontal drift chambers before and after a graphite analyzer. To minimize data processing bottlenecks, we plan to make a hardware cut on the second scattering angle to preselect events having a useful figure of merit. Figure 4 shows the focal plane electronics for the hadron arm.

Details of the spectrometers and instrumentation can be found in the Hall A Conceptual Design Report.[23]

5.1 Beam Time Summary

The total beam time needed for these measurements is shown in Table 12. Acquisition times are based on a luminosity of $2.8\times10^{38}\mathrm{cm}^{-2}\mathrm{sec}^{-1}$ and a beam polarization of 40%. Data acquisition times can be reduced by a factor of four if the beam polarization increases to 80%. The beam time estimate includes time for hydrogen normalizations, various other calibrations and tests and overhead associated with momentum and angle changes. The total time required for this experiment is 708 hours which would be reduced to 209 hours at the higher beam polarization.

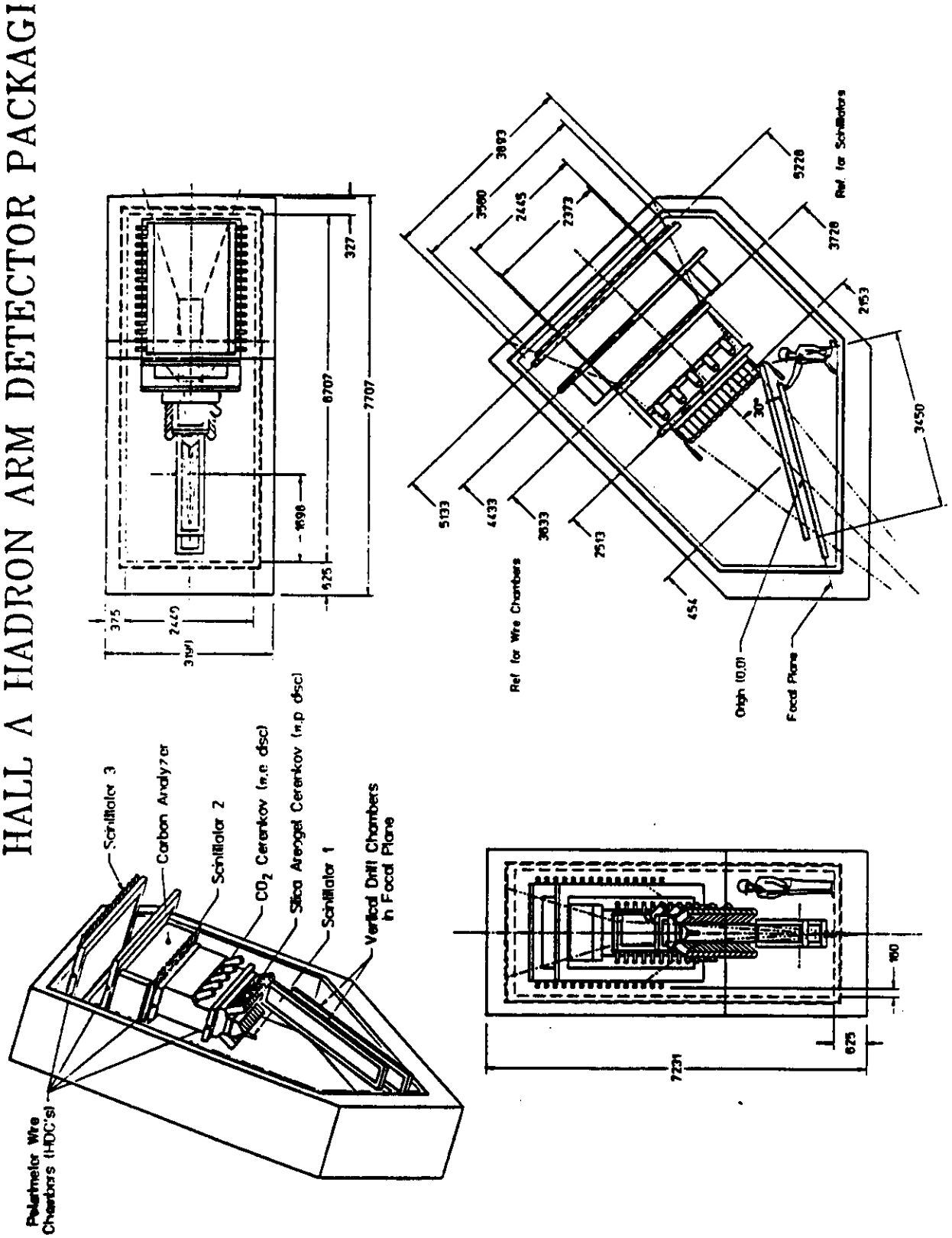

Figure 4 Schematic diagram of the focal plane instrumentation package for the hadron arm.

Table 12

Beam Time Summary

Measurement	time (hours) $L_{max} = 150\mu$A-g/cm^2
q_μ^2 dependence	248
Angular distribution	393
Hydrogen norm.	25
Tests and calib.	24
Angle/field changes	18
TOTAL at 40% polarization	708
TOTAL at 80% polarization	209

References

[1] S. Frullani and J. Mougey, *Advances in Nuclear Physics*, vol. 14, ed. by J.W. Negele and E. Vogt, Plenum Press (1985).

[2] T. de Forest, Jr., Nucl. Phys. **A392**, 232 (1983).

[3] T.W. Donnelly, MIT preprint no. CTP-1650 (1988); A.S. Raskin and T.W. Donnelly, MIT preprint no. CTP-1476 (1988).

[4] A. Picklesimer and J.W. Van Orden, Phys. Rev. C **40**, 290 (1989).

[5] R.G. Arnold, C.E. Carlson and F. Gross, Phys. Rev. **23**, 363 (1981).

[6] R. Madey *et al.*, *The Electric Form Factor of the Neutron from the* $D(\vec{e}, e'\vec{n})p$ *Reaction*, update of research proposal 85-05, submitted to the Bates Electron Accelerator Facility, (1987).

[7] H. Arenhövel, private communication.

[8] A.Yu. Korchin, Yu.P. Mel'nik and A.V. Shebeko, Sov. J. Nucl. Phys. **48**, 243 (1988).

[9] M.P. Rekalo, G.I. Gakh and A.P. Rekalo, J. Phys. G. **15**, 1223 (1989).

[10] J.W. Van Orden and F. Gross, private communication.

[11] Proposal submitted to CEBAF PAC4, C.F. Perdrisat and V. Punjabi, cospokespersons.

[12] A. Picklesimer and J.W. Van Orden, Phys. Rev. C**35**, 266 (1987).

[13] J.W. Van Orden, *Relativistic Effects and Spin Dependence in Electron Scattering*, to be published.

[14] J.W. Lightbody and J.S. O'Connell, Computers in Physics, May/June 1988, p. 57.

[15] L.E. Wright and L. Tiator, Phys. Rev. C **26**, 2349 (1982).

[16] A.E. Thorlacius and H.W. Fearing, Phys. Rev. C **33**, 1830 (1986).

[17] P.E. Ulmer, Program MCEEP (1989).

[18] F. Krautschneider, Ph.D. Thesis, Bonn University, BONN-IR-76-37 (1976); L. Hulthen and M. Sagawara, Handb. d. Phys. Bd. 39, S.1.

[19] M. Bernheim *et al.*, Nucl. Phys. **A365**, 349 (1981).

[20] M. Lacombe *et al.*, Phys. Lett. **101B**, 139 (1981).

[21] S.K. Nanda, *Proton Polarization Measurements in* $(\vec{e}, e'\vec{p})$ *with the HRS*^{2} *at CEBAF*, submitted to the CEBAF polarization workshop (1988) and to be published.

[22] C.F. Perdrisat, private communication.

[23] CEBAF Hall A Conceptual Design Report (1989).